

Morphological and morphometric characterisation of Onuf's nucleus in the spinal cord in man

A. H. PULLEN¹, D. TUCKER² AND J. E. MARTIN²

¹Sobell Department of Neurophysiology, Institute of Neurology, Queen Square, and ²Department of Neuropathology, Institute of Pathology, London Hospital Medical College, Whitechapel, London, UK

(Accepted 1 April 1997)

ABSTRACT

In the absence of a systematic morphometric study of Onuf's nucleus in man, this investigation defines the limits of variation of segmental position and the range of length and volume of Onuf's nucleus in 6 normal humans displaying no neurological disease (2 males, 4 females). Serial section reconstruction methods in conjunction with the disector method provided information on the numbers, sizes and shapes of the constituent motor neurons of Onuf's nucleus. In contrast to previous descriptions, the cranial origin of Onuf's nucleus occurred in rostral S1 in 50% of subjects, and midcaudal S1 in the remaining subjects. Onuf's nucleus varied in length between 4 and 7 mm, and was 0.2–0.37 mm³ in volume. Differences in length or volume between males or females, or between the left and right side of the cord were not statistically significant. Neurons in Onuf's nucleus varied in diameter between 10 µm and 60 µm (mean 26 µm) and their mean number was 625 ± 137. A higher density of neurons occurred at the cranial and caudal ends of the nucleus relative to the middle. While 37% of neurons were approximately spherical (shape index ~ 1), 44% were ellipsoid and 19% fusiform (shape indices varying between 0.26 and 0.8). These findings are compared with previous studies of Onuf's nucleus in man and animals. The results form a basis for further studies on Onuf's nucleus in normality and neurodegenerative diseases.

Key words: Motor neurons; sacral spinal cord.

INTRODUCTION

A distinct group of neurons in the sacral spinal cord in man located anteromedial to the anterolateral nucleus and extending between the distal part of S1 segment and the proximal part of S3 was identified by Onufrowicz (1889, 1890) as nucleus X. Subsequently, nucleus X was renamed Onuf's nucleus. Retrograde labelling experiments in cat, dog, rabbit and sub-human primates have identified homologues of Onuf's nucleus and shown them to innervate the external urethral and external anal sphincter muscles via the pudendal nerve (Sato et al. 1978; Nagashima et al. 1979; Kuzuhara et al. 1980; Roppolo et al. 1985). Anatomically and physiologically Onuf's nucleus is intriguing. It innervates striated muscle which is under voluntary control (Onufrowicz, 1890). The motor neurons are histologically similar to limb motor

neurons (Mannen et al. 1977) and possess the same 5 ultrastructural classes of presynaptic terminal as motor neurons innervating limb muscles, in particular the C-type axon terminal which is characterised by subsynaptic cistern and associated postsynaptic Nissl body. C-type terminals synapse only with somatic α-motor neurons and not Renshaw cells, gamma motor neurons, interneurons, or preganglionic parasympathetic neurons (Conradi, 1969; Lagerback & Ronnevi, 1982; Lagerback, 1985; Pullen, 1988; Johnson & Sears, 1988; Leedy et al. 1988; Pullen et al. 1992). Together, these features identify Onuf's nucleus as somatic but, curiously, the nucleus has some autonomic-like features, including a strong peptidergic presynaptic input (Schroder, 1984; Kawatani et al. 1986; Gibson et al. 1988; Tashiro et al. 1989), and a presynaptic input from midbrain nuclei which project both to Onuf's nucleus and autonomic preganglionic

parasympathetic intermediolateral neurons (Holstege & Tan, 1987). In neurological disease, Onuf's nucleus codegenerates with autonomic motor nuclei in the Shy-Drager syndrome (Sung et al. 1979) and progressive autonomic failure with multisystem atrophy (Kirby et al. 1986), but in amyotrophic lateral sclerosis which specifically kills somatic motor neurons, Onuf's nucleus is relatively spared (Mannen et al. 1977), although in some patients the motor neurons may exhibit cytoskeletal pathology (Pullen & Martin, 1995). Sexual dimorphism is a prominent feature of Onuf's nucleus in the rat (Breedlove & Arnold, 1981, 1983*a, b*) and dog (Forger & Breedlove, 1986), but evidence for dimorphism in man largely rests on difference in the total numbers of neurons in Onuf's nucleus of males and females (Forger & Breedlove, 1986).

Morphometric studies of lumbosacral motor neurons generally focus on limb motor neurons (e.g. Tomlinson et al. 1973; Irving et al. 1974). No report describes the overall size of Onuf's nucleus in man or the total numbers of the constituent neurons, or investigates their individual shapes. Since changes in these properties are one postmortem indicator of neurological disease, it is important to delineate the range of normality. At best, neuronal numbers in Onuf's nucleus have been estimated from studies of limited numbers of serial or semiserial sections, chiefly for comparison with similar sampling of histological sections from patients with neurological disease (e.g. Konno et al. 1986; Kihira et al. 1991; Sasaki & Maruyama, 1993). Such sampling possesses inherent errors which prevent accurate counts of total cell number and measurement of overall nucleus size. Sphincter motor neurons in Onuf's nucleus of man have been variously described as 'small' (Onufrowicz, 1890; Iwata & Hirano, 1978) or 'medium' (Mannen et al. 1977; Schroder, 1981), but these data are based on visual inspection of wax-embedded histological material without accompanying morphometry. Sizes of normal human sacral motor neurons have been measured in 'plastic' embedded sections of post-mortem spinal cord (Pullen et al. 1992), but differences in degrees of tissue preservation and methods of tissue preparation prevent projection of these data to routine histology. In most mammals, including man, Onuf's nucleus is generally divided into dorsomedial (DM) and ventrolateral (VL) regions (Sato et al. 1978; Kuzuhara et al. 1980; Schroder, 1981; Roppolo et al. 1985; Forger & Breedlove, 1986). However, other groups of neurons associated with the nucleus have been described emanating along its rostrocaudal axis (Rexed, 1954; Schroder, 1981). The exact number

and rostrocaudal location of such 'accessory nuclei' is unclear.

The aims of this study are to (1) analyse the anatomical architecture of Onuf's nucleus, (2) define the overall length and volume of the nucleus, (3) count the total of motor neurons in Onuf's nucleus, and (4) classify their shapes. To overcome the limitations provided by examinations of random sections at undefined levels through the nucleus, studies will employ serial sections encompassing the entire rostrocaudal length of the nucleus.

MATERIALS AND METHODS

Subjects

Spinal cords were collected with prior permission during routine postmortem examinations from 6 subjects, 4 females and 2 males. The mean age of the males was 63.3 y (range 55–64 y) and that of females was 65.3 y (range 59–72 y). Table 1 lists causes of death; none was neurological disease.

General protocol

The lower lumbar segments and S1, S2 and S3 were identified, removed with their corresponding nerve roots, and immersion-fixed in 10% formol saline solution for 12 h–24 h. Segmental boundaries were defined using the midpoint of the 1st sacral nerve root as the rostral reference point. The segments were embedded individually in paraffin wax using an automated Shandon–Elliot tissue processor and the following protocol. After immersion fixation, each segment was postfixed in 10% formol–alcohol (3 changes, 1 h, 2 h and 2 h), dehydrated in increasing percentages of industrial methanol (1 h in 70%, 1 h in 90%, 2 stages in 100%, 1 h each), cleared in toluene (3 changes, 1 h each), infiltrated with paraffin wax maintained at 54–56 °C (2 changes, 2 h and 3 h) and finally cast in paraffin wax. Serial transverse sections (10 µm) were cut along the entire rostrocaudal axis

Table 1. *Clinical details of cases studied*

Case no	Sex	Age (y)	Cause of death
1. 108/92	M	55	Dissecting aortic aneurysm
2. 201/92	M	64	Clivus meningioma
3. 241/92	F	59	Posterior fossa haemorrhage
4. 281/92	F	63	Dissecting aortic aneurysm
5. 286/92	F	61	Pulmonary embolus
6. 25/93	F	72	Congestive cardiomyopathy

of each segment and mounted in rostrocaudal order on coated microscope slides. The sections were stained with Luxol fast blue-cresyl fast violet using a modified Kluver & Barrera method to demonstrate and distinguish between, darkly blue-stained myelinated fibres traversing Onuf's nucleus, purple-stained Nissl substance and nucleoli in the neurons, and the unstained background.

Identification of Onuf's nucleus

Onuf's nucleus was identified by its position relative to the ventrolateral and ventromedial nuclei as defined in the original articles by Onufrowicz (1889, 1890) and by its distinctive morphology. This was characterised by (1) closely grouped neurons surrounded by a pale staining neuropil containing numerous cross-sectional profiles of axially oriented dendrites (Konishi et al. 1978; Takahashi & Yamamoto, 1979), and (2) a clearly discernible boundary marked by a sudden transition between the pale neuropil of Onuf's nucleus and the darker staining surrounding neuropil containing numerous longitudinal and obliquely sectioned myelinated axons, but no neurons.

This boundary region separated Onuf's nucleus from its neighbouring ventrolateral and ventromedial nuclei and was recognisable throughout the nucleus and in different subjects. It provided a defined morphological 'boundary' within which to acquire morphometric data, and in this respect, Onuf's nucleus is different from other more diffusely organised motor nuclei which, for data acquisition, require artificial boundaries to be set within the cross-sectional area of the nucleus.

Morphometry

The counts and measurements were made on each section. To examine possible left-right side differences each side of the cord was treated separately in the first instance. Data from both sides were subsequently pooled when differences were not statistically significant. The cross-sectional area of the nucleus was measured and counts of neurons were made on sections viewed with a $\times 10$ objective (final magnification $\times 100$).

(a) *Cross sectional area of Onuf's nucleus.* In each section, the boundary of the nucleus was identified (see above) and the maximum and minimum diameters of the nucleus were measured using an eyepiece graticule calibrated against a stage micrometer. The smallest detectable increment in nuclear diameter was 10 μm . Visually, the nucleus generally appeared ovoid,

and therefore its area was accordingly calculated using the formula:

$$\text{Area} = \Pi(a \times b)$$

where a and b are semiaxes, i.e. respectively, one half of the maximum and minimum diameters.

(b) *Overall length of Onuf's nucleus.* The total length of the nucleus was calculated by multiplying the total number of sections containing Onuf's nucleus by section thickness (10 μm = 0.01 mm). Segmental limits of the nucleus were defined with reference to the midpoint of the first sacral nerve root as outlined above.

(c) *Volume of the nucleus.* This was calculated in 3 stages. Firstly, the cross-sectional area encompassing Onuf's nucleus was calculated in each section as described above in (a). Secondly, the volume of the nucleus in each tissue section was calculated by multiplying the cross-sectional area by section thickness. Finally, the total volume of the nucleus was obtained by summing the individual volumes of the nucleus in each section over the number of sections containing the nucleus.

(d) *Numbers of motor neurons.* The total number of neurons contained within the boundary of Onuf's nucleus was counted using the disector method (Sterio, 1984; Pakkenburg & Gundersen, 1988). Briefly, neurons to be counted had to be present in the section under examination (the reference section), but not in the section immediately following the test section (the lookup sections). Since the same pair of sections can be examined in either a rostrocaudal or caudalrostral direction (Mayhew, 1992) the preceding section was rechecked to ensure profiles were not double counted. To further preclude 'split-cell' error arising from single neurons being represented in more than one section, valid neurons had to exhibit a nucleus with nucleolus. This protocol was chosen because it provides an unbiased sample which is free from assumptions concerning profile size and errors from estimation of reference volume (Sterio, 1984; Coggeshall, 1992). The method does not require the further corrections generally associated with biased methods entailing counts made on random sequences of serial or nonserial sections (e.g. Abercrombie correction factor).

(e) *Sizes of motor neurons.* The maximum and minimum diameters of each neuron conforming to the above inclusion criteria were measured using a calibrated eyepiece graticule and an $\times 25$ objective (final magnification $\times 250$). The smallest discernible increment in neuronal diameter was 0.5 divisions on the graticule (equivalent to 2.5 μm). Values were used

to calculate the mean diameter, sectional area, and perimeter of each neuron. Since most neurons tended to an ellipsoid shape, the following formulae were used.

$$\text{mean diameter} = \sqrt{\left(\frac{\text{maximum diameter} \times \text{minimum diameter}}{\text{diameter}}\right)}$$

$$\text{Area} = \Pi(a \times b),$$

where a and b are semiaxes (half values of maximum and minimum diameter.)

$$\text{Perimeter} = \Pi\sqrt{2[(a^2 + b^2)]},$$

where a and b are the semiaxes defined above.

(f) *Packing density of neurons.* This was determined for each section (= no neurons/ unit area of nucleus) using data in (a) and (d). The overall packing density for the entire nucleus was derived from measurements in (c) and (d).

(g) *Total number of neurons in the entire nucleus.* This was derived from summation of the individual data obtained for each section in (d).

(h) *Variation in the shape of motor neurons.* Motor neurons undergo alterations in shape following injury of their axons and in some neurodegenerative disease but not others (Kiernan & Hudson, 1993). To provide baseline data defining normality, shape indices were determined for each motor neuron. These were calculated in 2 ways: (1) as the ratio of maximum to minimum diameter (= 1 for a circular profile, > 1 for an ellipse); (2) using the classical shape index = $4\Pi(\text{area}/\text{perimeter}^2)$ (= 1 for a circle, < 1 for an ellipse).

Statistical analysis

Data sets obtained for the right and left hand nuclei of each subject were compared using paired-samples Student's t test and data sets for male and female subjects were compared with an unpaired t test. RHS and LHS data sets were pooled only if the differences were not statistically significant. In such cases the mean length and mean volume of the nucleus was determined, and also the mean neuronal count, mean neuronal diameter and neuronal shape (\pm S.D. and S.E.M.), and the differences retested with an unpaired Student's t test.

RESULTS

Location of Onuf's nucleus

A discrete group of neurons was identified in the extreme midventral region of the ventral horn at S2 in

each subject (Fig. 1). This group was located between a larger group situated ventrolaterally (the ventrolateral nucleus; VL), and a smaller group in the ventromedial tip of the ventral horn (the ventromedial nucleus; VM) and conformed to the positions of nucleus X described by Onufrowicz (1890) and Onuf's nucleus reported by Schroder (1981). Onuf's nucleus (ON) is illustrated in relation to the VL and VM nuclei in Figure 1e. Although the origin of Onuf's nucleus was within the 1st sacral segment in all 6 subjects, in 3 subjects the nucleus was first detected in rostral S1, but midcaudal S1 in the remaining subjects (Fig. 2a). Onuf's nucleus varied in its dorsoventral position along its rostrocaudal axis. In more rostral levels, the nucleus formed a separate group of neurons located in the ventral region of the ventral horn, midway between the medial and lateral motor nuclei (Fig. 1a). At more caudal levels, the nucleus was displaced ventrally, to be situated immediately adjacent to the boundary between grey and white matter at the region where the efferent tracts emerge from the grey matter (Fig. 1b).

Architecture of Onuf's nucleus

The main nucleus. Individual sections generally showed Onuf's nucleus to be round to oval in cross-section (Fig. 1a). Cross-sectional area was maximal near its midlength and reduced towards its rostral and caudal ends, suggesting that the nucleus was generally 'cigar-shaped' (best illustrated by reference to Fig. 3b). The overall shape of Onuf's nucleus was closely similar on the left and right sides of the cord. Internally, groups of motor neurons separated by neuropil or myelinated fibres were seen in some transverse sections which gave the appearance of a multilobed structure (Fig. 1c, d). This appearance was particularly prominent in the midaxial region of Onuf's nucleus (S2), where the nucleus was divided into 2 distinct groups of neurons; a 'medial' to 'dorsomedial' group, and a ventrolateral group which were separated by an intervening bundle of myelinated nerve fibres of no fixed orientation (Fig. 2d). The 2 groups merged at the rostral and caudal levels of the nucleus.

Associated structures. While the main volume of the nucleus formed a continuous structure, the contour of the nucleus was often modified at its midregion and at its rostral and caudal ends by groups of neurons extending away from the main body of the nucleus, suggesting the presence of 'accessory nuclei'. To provide a practical criterion for identifying an 'accessory nucleus', such a nucleus was present if a

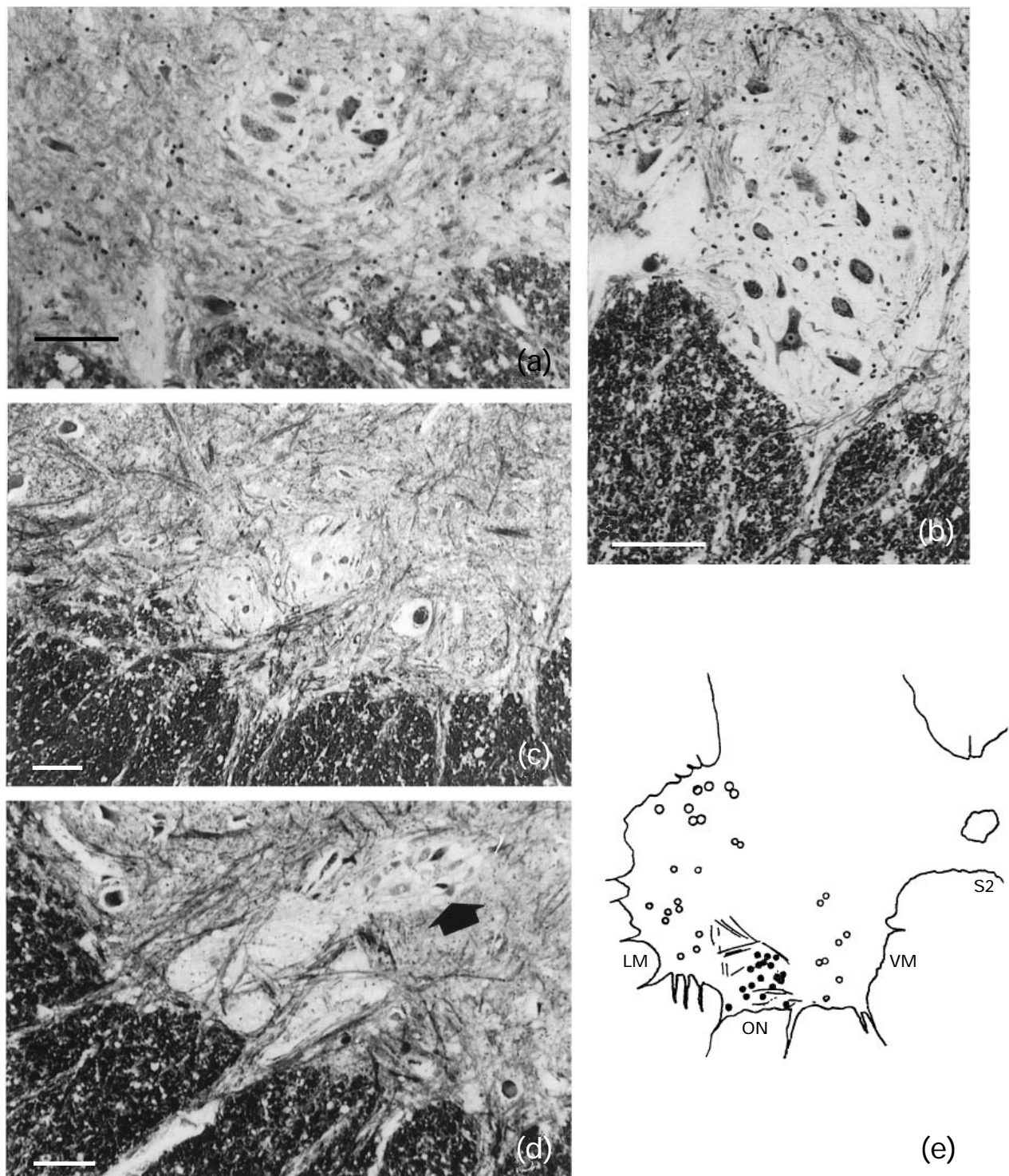


Fig. 1. Onuf's nucleus in luxol fast blue-cresyl violet stained histological sections. (a), cranial region; (b), caudal region; (c), midlongitudinal region showing bisection by myelinated fibres; (d), different aspect of the midlongitudinal region of Onuf's nucleus showing its division by myelinated fibres producing a dorsomedial group of neurons (arrow) and a more ventral group; (e), diagram of the relative positions of Onuf's nucleus (ON) and the ventrolateral (VL) and ventromedial nuclei (VM) as seen in S2. Bars, *a-d*, 100 μ m.

distance of more than 100 μ m separated the main volume of the nucleus from the additional group of neurons. The relative numbers of accessory nuclei of the right and left sides of each subject are compared in Fig. 2*b*.

Size of Onuf's nucleus

Length. The overall length of the Onuf's nucleus was taken as the main nucleus plus any rostral and/or caudal 'accessory nuclei'. Lengths for individual

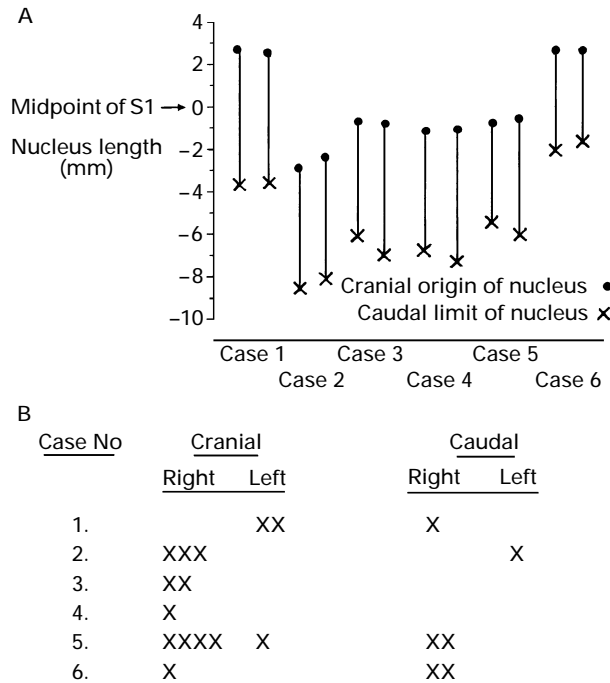


Fig. 2. (A) Comparison of the cranial origins and segmental representations of Onuf's nucleus relative to the midpoint of the S1 segment. (B) Comparative distribution and number of rostral and caudal accessory nuclei associated with Onuf's nucleus on the right and left sides of the sacral spinal cord.

subjects are summarised in Table 2. The lengths of Onuf's nucleus on the right and left side of the cord were similar. Since the small differences were not statistically significant ($t = 1.573$, D.F. = 5, $P > 0.1$, paired 2-sample t test), data for the RHS were pooled and compared with pooled data for the LHS. Differences in the overall length of Onuf's nucleus on the RHS and LHS were not significant (RHS, mean = 5.88 ± 0.78 mm; LHS, mean = 6.08 ± 1.11 mm, $t = 0.3688$, $P > 0.1$, unpaired Student's t test). The overall mean length calculated by pooling data from right and left sides of individual subjects was 5.98 ± 0.926 mm (range 4.03–7.29 mm). The lengths of rostral accessory nuclei ranged between 90 and 500 μ m (mean 265 ± 183 μ m), and caudal accessory nuclei measured 40–620 μ m (mean 235.2 ± 160 μ m). The length of Onuf's nucleus was similar in male and female subjects. In males it was 6.582 ± 0.514 mm, and, 5.680 ± 0.959 mm in females ($P = 0.1075$, unpaired 2-tailed t test).

Volume. The volumes of the Onuf's nuclei on the left and right hand sides of individual subjects are compared in Table 2. The differences in volumes between the two sides were not statistically significant for individual subjects (paired t test; $t = 0.238$, D.F. = 5, $P > 0.1$); therefore, data for the RHS was pooled and compared with pooled data for the LHS. The

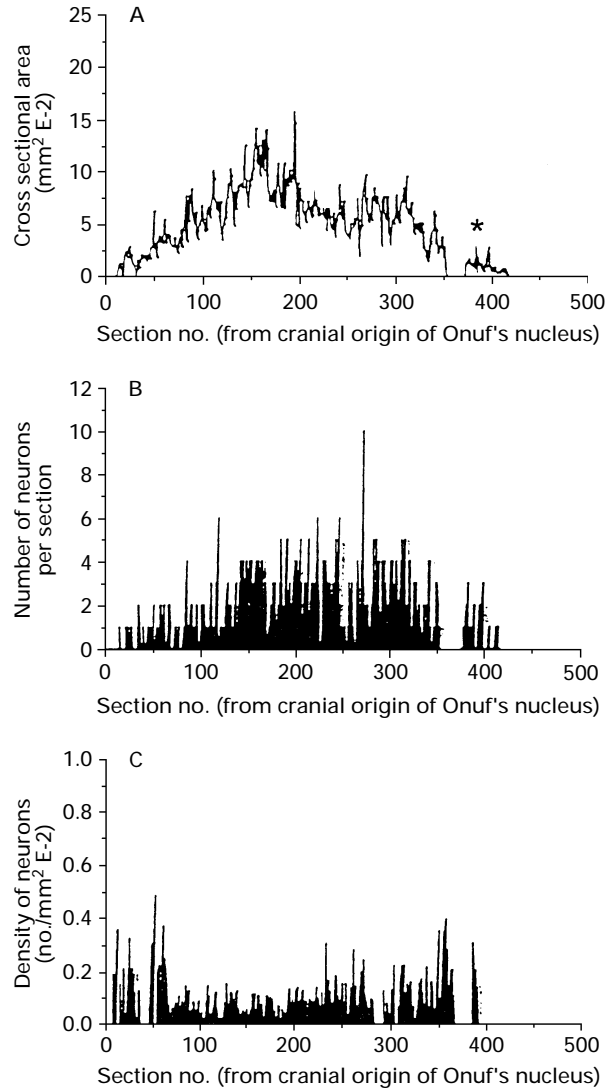


Fig. 3. Variation in the cross-sectional area (A), numbers of neurons (B) and density of neurons (C) along the rostrocaudal axis of Onuf's nucleus illustrated in subjects 3 and 5. The neuronal content of Onuf's nucleus varies along its length. At its midlength, the cross-sectional area and number of neurons are both maximal, but because neurons in this region are larger, relative to the rostral and caudal ends of the nucleus, the density of neurons (no./unit area) is lower than at the extremities of the nucleus.

Table 2. Comparison of the length, volume and number of neurons in Onuf's nucleus on the right and left side of the sacral spinal cord

Case no.	Length of nucleus (mm)		Volume of nucleus ($\text{mm}^3 \times 10^{-3}$)		Number of neurons	
	RHS	LHS	RHS	LHS	RHS	LHS
1	6.26	6.15	294.76	252.85	635	525
2	6.63	7.29	300.01	336.36	603	856
3	5.99	6.43	275.91	303.00	445	557
4	5.64	5.92	370.14	344.87	548	539
5	6.33	6.88	277.05	264.5	823	840
6	4.42	4.03	198.22	234.51	597	538

overall volume of the nucleus on the left side of the cord was $0.286 \pm 0.0556 \text{ mm}^3$, and for the right side $0.292 \pm 0.045 \text{ mm}^3$. Differences were not statistically significant (unpaired *t* test; $t = 0.2030$, D.F. = 10, $P > 0.1$). The overall mean volume of the nucleus calculated by pooling LHS and RHS data was $0.289 \pm 0.048 \text{ mm}^3$ (range 0.2–0.371 mm^3). In male subjects, the mean volume of the nucleus inclusive of the accessory nuclei was $0.299 \pm 0.0369 \text{ mm}^3$ and in females $0.285 \pm 0.0551 \text{ mm}^3$. However, because sample sizes were small, the statistical level of significance in differences between the volume of the nucleus in male and females ($t = 0.448$, D.F. = 10, $P > 0.1$) must be interpreted with caution.

Number of neurons

Identity of the neurons. Retrograde labelling is not possible in the human cadaver, but in the cat and monkey retrograde labelling procedures demonstrate that *all* neurons in Onuf's nucleus acquire label following intramuscular injections of HRP or other tracers (Sato et al. 1978; Roppolo et al. 1985), indicating the nucleus contains α - and γ -motor neurons. The lack of unlabelled neurons suggests interneurons do not occur. In Shy-Drager disease weakness of pelvic floor and sphincter muscles is associated with degeneration of neurons in Onuf's nucleus (Sung et al. 1979; Konno et al. 1986). Together, these lines of evidence indicate that Onuf's nucleus contains motor neurons.

Total number of neurons in nucleus. The total numbers of neurons counted on each side of the spinal cord in individual subjects are given in Table 2. Numbers of neurons were similar on both sides of the cord in individual subjects, and a paired *t* test revealed that differences between the two sides of the cord were not statistically significant ($t = 0.633$, D.F. = 5, $P > 0.1$). Overall, the numbers of neurons on the right side of the cord were 608 ± 124.3 (RHS), and on the left 642 ± 159 (LHS). The difference was not significant; $t = 0.417$, D.F. = 10, $P > 0.1$ (unpaired *t* test). On pooling data from both sides of the cord for all 6 subjects, the mean number of motor neurons was 625 ± 137 (range 445–856). The mean number of motor neurons in Onuf's nucleus of male subjects was 654 ± 141.8 , but slightly lower in females, 610 ± 142.7 . Although statistically the difference was not significant ($t = 0.502$, D.F. = 10, $P > 0.1$), a larger sample would be required to provide a secure conclusion regarding possible sexual dimorphism.

Numerical distribution. In Onuf's nucleus of the cat

neurons are grouped in clusters linked by axial bundles of dendrites (Thor et al. 1989). In man there is little information regarding the rostrocaudal distribution of neurons in Onuf's nucleus even though such information could influence interpretation of histopathology specimens from subjects with degenerative diseases affecting sacral somatovisceral systems. Therefore the longitudinal variation in cross-sectional area of Onuf's nucleus was determined, and related to the longitudinal distribution of neurons. As illustrated in Figure 3*a*, the cross-sectional area of Onuf's nucleus was maximal near its midaxis and reduced towards both cranial and caudal limits. The number of neurons within Onuf's nucleus in a section also varied along the rostrocaudal axis, with the highest numbers being found at the midaxial region (typically 4–8; Fig. 3*b*), and reduced to 1–3 neurons at rostral and caudal poles. Due to differences in neuronal diameter along the axis of the nucleus (see below), the density of neurons (no./unit area) was slightly higher at the rostral and caudal ends of the nucleus than at the midaxial region (Fig. 3*c*). This pattern of distribution in Onuf's nucleus was identical on both the right and left sides of the cord, and in all subjects.

The implication of Figure 3 is that in assessing possible neuronal loss in neurodegenerative diseases, it is important to consider the particular rostrocaudal level of the histological section.

Size of motor neurons (diameter/area)

The smallest neurons and glial cells of similar size were distinguished by their different morphologies. Motor neurons were distinguished on the basis of their prominent cresyl violet stained cytoplasmic basophilic Nissl bodies and a pale staining nucleus containing an intensely stained nucleolus. By contrast, glia were identified by their larger nucleus containing densely stained blocks of chromatin, and a thin 'rim' of cytoplasm which was devoid of basophilic 'patches' (Nissl bodies). Similar criteria have been used elsewhere (Bjgun & Gundersen, 1993).

The mean diameters and cross-sectional areas of motor neurons measured in Onuf's nucleus are given for individual subjects in the upper section of Table 3. Statistical analysis did not detect any significant differences in mean neuronal diameter between the left and right hand side nuclei in these subjects ($t = 1.502$, D.F. = 5, $P < 0.2 > 0.1$ paired 2-sample *t* test), nor for the overall population ($t = 0.459$, D.F. = 10, $P > 0.1$). Likewise, differences between the cross-sectional areas of motor neurons in Onuf's nucleus on

Table 3. Comparison of the mean diameter, cross-sectional areas and shape indices of motor neurons in Onuf's nucleus of 6 subjects who have no neurological disease of the sacral spinal cord

Case no.	RHS					LHS				
	n	Range	Mean	S.D.	S.E.	n	Range	Mean	S.D.	S.E.
(a) Diameters of motor neurons in Onuf's nucleus of the neurologically normal human										
1	635	12.2–54.5	30.01	7.58	0.3	525	12.2–57.0	27.93	7.31	0.32
2	603	10.0–37.1	22.3	4.5	0.18	856	12.2–41.8	23.52	4.83	0.17
3	445	14.1–45.8	25.6	5.4	0.26	557	12.2–43.3	24.3	4.81	0.20
4	548	10.0–44.7	23.5	5.3	0.23	539	12.2–43.9	23.7	5.42	0.23
5	823	14.1–50.9	28.6	5.8	0.2	840	12.0–70.7	27.7	6.43	0.22
6	597	14.1–48.9	30.0	6.5	0.27	538	12.2–50.9	28.23	6.6	0.28
(b) Sectional areas of motor neurons in Onuf's nucleus of the neurologically normal human										
1	635	117.8–2336.9	752.5	374.8	14.87	525	117.8–2552.8	654.4	351.2	15.33
2	603	75.5–1080.1	406.7	165.6	6.74	856	117.8–1374.6	452.9	190.8	6.52
3	445	157.1–1649.6	538.4	238.9	11.33	557	117.8–1472.8	482.1	196.9	8.34
4	548	23.6–1571.0	455.2	209.7	8.96	539	117.8–1512.1	465.3	215.6	9.28
5	823	157.1–2042.3	667.2	272.9	9.51	840	117.8–3927.5	640.0	306.6	10.58
6	597	157.1–1885.2	740.9	311.8	12.76	538	117.8–2042.3	658.1	200.9	12.98
(c) Values of shape index for motor neurons in Onuf's nucleus of the neurologically normal human										
1	635	0.38–1.0	0.84	0.13	0.01	525	0.28–1.0	0.83	0.14	0.01
2	603	0.35–1.0	0.88	0.11	0.004	856	0.35–1.0	0.88	0.12	0.004
3	445	0.60–1.0	0.92	0.08	0.004	557	0.38–1.0	0.91	0.10	0.004
4	548	0.07–1.0	0.88	0.11	0.005	539	0.42–1.0	0.89	0.11	0.005
5	823	0.38–1.0	0.87	0.12	0.004	840	0.25–1.0	0.87	0.12	0.004
6	597	0.26–1.0	0.86	0.13	0.005	538	0.25–1.0	0.87	0.12	0.005

the RHS and LHS were not significant ($t = 1.53$, D.F. = 5, $P < 0.2 > 0.1$; paired 2-sample t test). Pooled data from all 6 subjects provided an overall mean neuronal diameter of $26.62 \pm 2.66 \mu\text{m}$ (range 10–60 μm), and a mean cross-sectional area of $576.14 \pm 122.32 \mu\text{m}^2$ (range 23.6–2336.9 μm^2). Mean neuronal sizes of male and female subjects were very similar (males; $25.94 \pm 3.63 \mu\text{m}$, females; $26.25 \pm 2.25 \mu\text{m}$, $t = 0.608$, 10 D.F., $P = > 0.1$). Since some previous published data cite minimum diameters because these are least subject to error caused by variation in section orientation, the mean minimum diameters were also calculated for the subjects examined here. The range and overall mean minimum diameters of neurons in Onuf's nucleus was 7.5–55 μm ($21.05 \pm 5.93 \mu\text{m}$). In these measurements no differences between left and right nuclei or between sexes were detected (e.g. LHS–RHS difference, $P > 0.1$, 95% confidence limits $20.90 \leq \text{mean} \leq 21.20$, range 5–55).

Shape of motor neurons. Neuronal hypertrophy confers increased circularity to neurons; conversely, atrophy is characterised by polymorphism. To provide a baseline for assessment of altered shape in disease, neuronal shape was examined in these normal subjects. Motor neurons in Onuf's nucleus ranged between approximately circular through ellipsoid to elongated spindle shaped. Circular neurons accounted for 37% (indices 0.85–1.0), ellipsoid 44% (0.6–0.85),

and 19% were fusiform (shape indices < 0.6). The latter shaped neurons appeared in many sections, but not all, and were generally smaller than motor neurons in the ventromedial and ventrolateral motor nuclei. The lower section of Table 3 summarises the ratios of the maximum to mean neuronal diameters and the shape indices for individual subjects. The mean neuronal shape index was identical on both sides of the cord (0.875 ± 0.0266 , range 0.26–1.00) and was similar in males and females (males, 0.875 ± 0.0262 , females 0.883 ± 0.0212 , $t = 0.6203$, D.F. = 10, $P > 0.1$).

DISCUSSION

The qualitative and morphometric characterisation of Onuf's nucleus in the neurologically normal human has provided a number of original data for the range and mean length and volume of the nucleus, and the variation in size, density and shape of the constituent neurons. The data enable both a general scientific insight into this unique nucleus, and a practical base for defining alterations in this nucleus imposed by neurological disease.

The disector method (Sterio, 1984) for counting profiles used here in combination with serial section reconstruction has major advantages over techniques

entailing sampling of nonserial sections with subsequent estimation of profile number and tissue volume (see Coggeshall, 1992). These include freedom from assumptions that a given section truly represents all other sections, that the relative sizes of profiles in the sample section reproduce the true range of sizes present in the volume of tissue, and that application of correction factors (e.g. Abercrombie correction) to acquired data either minimise or eliminate error. The disector protocol yields an absolute numerical count which provides a reference for comparing data reported elsewhere and obtained with other sampling-based methods. The disector technique identifies and counts 'tops' (cross-sectional profiles through a particle) seen in a section only if they do not also appear in an adjacent 'lookup' section (Sterio, 1984); the method produces an unbiased population sample of counted or measured profiles. Detailed analysis of Case 1 showed about 16% of sections failed to exhibit any neuronal structure, 23% contained a single neuronal profile possessing a nucleus, 14% exhibited 2 profiles with a nucleus, and 15% had 3–6 profiles with a nucleus. About 1.5% of sections contained 7–8 such profiles. The remainder of sections contained neuronal profiles outside a nuclear plane of section. Typically, neurons ranged between 30 and 70 μm in diameter, possessed a nucleus 15 μm in diameter, and a nucleolus 3–6 μm in diameter. At 10 μm section thickness, parallel planes through a single neuron may span up to 8 sections, the nucleus may occur in up to 3 sections, but the nucleolus in a maximum of 2 sections (Tomlinson et al. 1973; Irving et al. 1974). Double-counting of the nucleolus may be eliminated by the disector technique. Residual error in size measurements largely derives from postmortem autolysis and subsequent shrinkage during immersion fixation and histological processing. Tomlinson et al. (1973) estimated shrinkage to be 20–25%. In this study it is therefore possible that the length and volume of the Onuf's nucleus under-represents the *in vivo* dimensions. The method for processing and staining of tissue used here is routine and used in many pathology departments. The histological data should be comparable with those from other laboratories. To further eliminate such artifacts would require the use of unfixed frozen sections; however the practical difficulties associated with snap-freezing of unprotected postmortem tissue equivalent in volume to 2–3 spinal segments would make this a difficult procedure to achieve.

Regarding the morphological findings, in this study Onuf's nucleus originated in S1 in all 6 subjects and extended caudally into S2. In 3 subjects the origin

occurred in mid-S1, whereas Onufrowicz (1889, 1890) originally reported nucleus 'X' to originate in caudal S1, and while he found it extended caudally into rostral S3 of some subjects, he noted it was particularly characteristic of S2. The later study of parasagittal sections from 59 normal subjects by Schroder (1981) similarly found Onuf's nucleus to span S1–S3, with its major volume in S2 and S3, and a sparse representation in S1. Lareulle (1937) examined longitudinal sections of human sacral cord, reporting a similar segmental representation. These different accounts suggest Onuf's nucleus in man exhibits a certain degree of segmental rostrocaudal variation in its location. An analogous variation occurs in animals. In the cat and rabbit segmental representation is similar to that of man. In the rabbit, retrograde labelling methods show motor neurons innervating the external anal sphincter occur between rostral S2–mid S3 (Nagashima et al. 1979). In the cat, labelled sphincter motor neurons first arose midcaudal S1, became most numerous in rostral S2, and showed marked reduction in number in caudal S2, and did not extend into S3 (Sato et al. 1978; Takahashi & Yamamoto, 1979; Pullen, 1988). Ueyma et al. (1985) noted that out of 13 macaques, motor neurons in Onuf's nucleus with efferents in the pudendal nerve spanned a region from rostral–mid S1 to rostral–mid S2 in 8 animals, originated in midcaudal L7 and terminated in rostral S2 in 4 animals, and in 1 animal originated in rostral L7, terminating at mid-S1. By contrast, Roppolo et al. (1985) identified Onuf's nucleus in the Rhesus monkey to occupy L7–S1, which is similar to the lumbosacral location (L6–S1) found in rat by Schroder (1980).

Length of Onuf's nucleus

The range of length of Onuf's nucleus in these subjects, 4–7 mm, is similar to that reported by Schroder (1981) (3.5–7.9 mm), but Forger & Breedlove (1986) found the nucleus to be slightly shorter (~ 3.5 mm). The similarity in length of nucleus in left and right sides of the cord found here agrees with Schroder's observations. The lack of difference in length of the nucleus between males and females noted here agrees with the finding by Forger & Breedlove (1986) but requires further confirmation using larger sample sizes. Schroder (1981) observed a significant variation in length of Onuf's nucleus between individuals, but unfortunately failed to correlate length with sex. In relation to other species, in cat the length of Onuf's nucleus is similar to that in man (2.6–8 mm; Thor et al. 1989; Sasaki &

Murayama, 1993), but in the macaque it is longer (7.5–11.4 mm, mean 9.3 mm; Roppolo et al. 1985).

Volume

No previous studies report the volume of Onuf's nucleus in man, precluding a comparison with previous data. The lack of apparent differences in the total volume of Onuf's nucleus between males and females found here may more reflect insufficient subject numbers rather than a true lack of dimorphism. By contrast, volumetric differences do occur between the sexes in the canine homologue of Onuf's nucleus (Forger & Breedlove, 1986) where in males it is 2.2 times larger than in females. Interspecies variation in dimorphism is likely to be due to a combination of differences in the efferent projection of Onuf's nucleus, and reproductive behaviour.

Variation in relative position within the ventral horn

Onufrowicz (1889, 1890) interpreted nonsequential sections through L5, S1 and S2 identified nucleus 'X' as a separate group of neurons in S2 at a position formerly occupied by the anterolateral nucleus which terminated in S1. The more medioventral position of nucleus X at the midventral border between white and grey matter, and between the posterolateral and anteromedial nuclei, suggested to Onuf that the nucleus altered its position with respect to other nuclei along its rostrocaudal axis. The serial section reconstruction technique used here has enabled the relative 'shift' of Onuf's nucleus in relation to the central canal and white matter of the spinal cord to be documented along its rostrocaudal length. In mid-caudal S1, the nucleus originated in the medial region of the ventral horn and 'migrated' ventrally to the junction of the grey and white matter with caudal progression through S1 to S2 (Fig. 1*a, b*). Schroder (1981) noted that Onuf's nucleus was situated at the ventral border of the ventral horn in caudal S2, but in rostral S2, a pronounced region of grey matter was interposed between the nucleus and the white matter, suggesting a more dorsal location. A similar shift position of this nucleus along its rostrocaudal axis also occurs in the monkey (Roppolo et al. 1985) and cat (Sato et al. 1978). In the cat, the nucleus shifts ventromedially from a medial position in the intermediate ventral horn at S1, to occupy a midventral position adjacent to the white matter in mid-S2. Here it assumes a position midway between the large

ventrolateral nucleus and considerably smaller ventromedial nucleus (Sato et al. 1978).

Internal architecture of Onuf's nucleus

The 2 spatially separate groups of neurons found here in Onuf's nucleus, separated by a bundle of myelinated fibres appears characteristic of the midaxial region of this nucleus. The medial to dorsomedial group described here corresponds to the DM group described by Schroder (1981) and Forger & Breedlove (1986), and the more ventral group corresponds to the VL group as described by Schroder and Forger & Breedlove. Nerve fibres traversing Onuf's nucleus have also been observed in Onuf's nucleus in the cat (Pullen, 1988) and in man (Schroder, 1981). Pullen et al. (1992) reported that Onuf's nucleus in man formed a 'single unified group of neurons and was not subdivided by a prominent diagonal bundle of myelinated fibres'. However, the findings in this study indicate that the ultrastructural examination focused on either a rostral or caudal level of the nucleus where a single undivided structure occurs. For completeness, it is worth noting that the DM and VL nuclei in the rat are spatially separated throughout the longitudinal axis of the nucleus. The VL is located in a position resembling that of the entire nucleus in man, but the DM component is located at the medial border between grey and white matter ventral to the central canal (Schroder, 1980).

Accessory nuclei

Cranial accessory nuclei associated with Onuf's nucleus in man were first described by Schroder (1981), and were again identified in this study in 3 of the 6 subjects, suggesting accessory nuclei are a characteristic of Onuf's nucleus. Our work demonstrated caudal accessory nuclei. To our knowledge this is the first time such a group has been described, which is surprising since they occurred more frequently than rostral accessory neurons (Table 2). The presence and number of 'accessory nuclei' did not appear dependent on sex, length of Onuf's nucleus, or the presence of an 'accessory nucleus' on the opposite side of the cord. No correlations were discernible between the number of accessory nuclei and other morphological features of the nucleus. In the absence of physiological studies of these neurons it is not possible to attribute a function different from that of neurons in the main nucleus. There are no published reports of

similar accessory nuclei in other species, although Rexed (1954) described a small line of 'bridging cells' in the cat apparently connecting Onuf's nucleus and the preganglionic parasympathetic nucleus.

Neuronal sizes

Previous investigations of neuronal size in Onuf's nucleus have been qualitative and generally describe the neurons as 'small', or 'medium' (e.g. Onufrowicz, 1890; Mannen et al. 1977; Iwata & Hirano, 1978; Schroder, 1981). The quantitative ultrastructural study by Pullen et al. (1992) calculated a mean motor neuron diameter of $38.8 \pm 12.8 \mu\text{m}$, and found some neurons were similar in size to motor neurons subserving limb muscles. Using criteria derived from physiological convention, Pullen et al. (1992) classified neurons $< 30 \mu\text{m}$ to be 'small' and within the range associated with mammalian gamma motor neurons (Strick et al. 1976; Ulfhake & Kellerth, 1981 *a, b*), and those $> 30 \mu\text{m}$ to be large and of a range associated with alpha motor neurons. On that basis, neurons in Onuf's nucleus spanned the 'small' to 'large'. In this histological study, the mean neuronal diameter of $26 \mu\text{m}$ places neurons in the 'small' category, and the overall range between 'small' and 'medium' ($35\text{--}45 \mu\text{m}$). Differences in motor neuron size between the two studies may be due to a greater degree of tissue shrinkage seen with histological preparation ($\sim 25\%$; Tomlinson et al. 1973), relative to electron microscopy where preparative fixatives and buffers are near iso-osmotic and their relative ionic balances are carefully maintained throughout tissue preparation. Enhanced shrinkage by the particular histological procedure used here is unlikely: the protocol is identical to that used in most laboratories. The distribution of neuronal diameters (not illustrated) showed a single maximum (i.e. unimodal) with a continuum of size between the limits. No clear evidence was obtained of different populations of neurons being distinguishable on the basis of diameter, as suggested by Lareulle (1937). However, analyses of neuronal shape revealed distinct groups of neurons which conformed to fusiform, ellipsoid, and round. The functional significance of this variation is obscure, but alterations of neuronal shape occur in neuropathology (Kiernan & Hudson, 1993) and the present data provide a useful morphometric baseline defining normality. Neuronal areas measured here (mean $625 \mu\text{m}^2$) were similar to those previously reported for Onuf's nucleus in nonneurological subjects (e.g. mean area = $656 \mu\text{m}^2$, Kihira et al. 1991, and $529 \mu\text{m}^2$, Kiernan & Hudson, 1993).

Neuronal numbers and distribution

This is the first quantitative report of the total numbers of motor neurons in Onuf's nucleus of the normal human, and the first quantitative analysis of the numbers of motor neurons at different levels along its rostrocaudal axis. Our demonstration that neurons are more numerous at the midlength of the nucleus than at its rostral and caudal poles agrees with the original qualitative description by Onufrowicz (1889, 1890) which indicated neurons in nucleus X increase in number from the origin to the midpoint, and thereafter reduce towards the caudal pole. No qualitative assessment of neuronal number along the axis of the nucleus was made by Schroder (1981). This study also newly demonstrates that neuronal packing density is greater at the rostral and caudal ends of the nucleus than at its centre. Cross-sectional area of the nucleus apart, one component of the variation in density along the nucleus is the larger diameter of neurons in the dorsomedial component of the nucleus which is most prominent midway along the nucleus (Schroder, 1981). In the cat, neuron numbers also decrease in Onuf's nucleus towards the caudal end of S2 (Sato et al. 1978).

Regarding overall numbers of neurons in Onuf's nucleus in man, no significant difference was found either between left and right hand sides of the cord, or between males and females. The latter observation however requires cautious interpretation since the sample is small and requires enlarging to provide unequivocal evidence of sexual dimorphism. Using a larger number of subjects and wider age-range (1.5–87 y), Forger & Breedlove (1986) noted a larger number of neurons in males probably associated with the bulbocavernosus and ischiocavernosus muscles.

The new data provided by these studies provide a baseline for comparative anatomical aspects of sacral spinal cord morphology. The new morphometric data describing the normal anatomy of a special group of motor neurons in Onuf's nucleus of normal human subjects in the absence of motor neuron disorders (neurodegenerative disease) may also be useful in investigating the interesting responses of this group of motor neurons to neurological diseases such as the Shy-Drager form of multiple system atrophy and amyotrophic lateral sclerosis.

ACKNOWLEDGEMENTS

D.T. completed this study as part of an intercalated Bachelor of Science degree in experimental pathology and was supported by the Tallow Chandlers Com-

pany. J.E.M. is a Wellcome Trust Fellow. Our work is supported by the Motor Neuron Disease Association of Great Britain and the Wellcome Trust.

REFERENCES

- BJUGN R, GUNDERSEN HJR (1993) Estimate of the total number of neurons and glial and endothelial cells in the rat spinal cord by means of the optical disector. *Journal of Comparative Neurology* **328**, 406–414.
- BREEDLOVE SM, ARNOLD AP (1981) Sexually dimorphic motor nucleus in the rat lumbar spinal cord: response to adult hormone manipulation, absence in androgen insensitive rats. *Brain Research* **225**, 297–357.
- BREEDLOVE SM, ARNOLD AP. (1983a) Hormonal control of a developing neuromuscular system I: Complete demasculinisation of the spinal nucleus of the bulbocavernosus in male rats using the anti-androgen flutamide. *Journal of Neuroscience* **3**, 417–423.
- BREEDLOVE SM, ARNOLD AP (1983b) Hormonal control of a developing neuromuscular system II: Sensitive periods for the androgen induced masculinisation of the rat spinal nucleus of bulbocavernosus. *Journal of Neuroscience* **3**, 424–432.
- CONRADI S (1969). Ultrastructure and distribution of neuronal and glial elements on the motoneurone surface in the lumbosacral spinal cord of the adult cat. *Acta Physiologica Scandinavica* (Suppl.) **332**, 5–48.
- COGGESHALL RE (1992) A consideration of neural counting methods. *Trends in the Neurosciences* **15**, 9–13.
- FORGER N, BREEDLOVE SM (1986) Sexual dimorphism in human and canine spinal cord: role of early androgen. *Proceedings of the National Academy of Sciences of the USA* **83**, 7527–7531.
- GIBSON S, POLAK JM, KATAGIRI T, SU H, WELLER RO, BROWNELL DB et al. (1988) A comparison of the distribution of eight peptides in spinal cord from controls and cases of motor neurone disease with special reference to Onuf's nucleus. *Brain Research* **474**, 255–278.
- HOLSTEGE G, TAN J (1987) Supraspinal control of motoneurons innervating the striated muscles of the pelvic floor including urethral and anal sphincters in the cat. *Brain* **110**, 1323–1344.
- IRVING D, REBEZ JJ, TOMLINSON BE (1974) The numbers of limb motor neurones in the individual segments of the human lumbosacral spinal cord. *Journal of the Neurological Sciences* **21**, 203–212.
- IWATA M, HIRANO A (1978) Sparing of the Onufrowicz nucleus in sacral anterior horn lesions. *Annals of Neurology* **4**, 245–249.
- JOHNSON IP, SEARS TA (1988) Ultrastructure of interneurons within motor nuclei of the thoracic region of the spinal cord of the adult cat. *Journal of Anatomy* **161**, 171–185.
- KAWATANI M, NAGEL J, DEGROAT WC (1986). Identification of neuropeptides in pelvic and pudendal afferent pathways to the sacral spinal cord of the cat. *Journal of Comparative Neurology*, **249**, 117–132.
- KIERNAN JA, HUDSON AJ (1993) Changes in shapes of surviving motor neurons in amyotrophic lateral sclerosis. *Brain* **116**, 203–215.
- KIHIRA T, YOSHIDA S, UEBAYASHI Y, YASE Y, YOSHIMASU F (1991) Involvement of Onuf's nucleus in ALS—demonstration of intraneuronal conglomerate inclusions and Bunina bodies. *Journal of the Neurological Sciences* **104**, 119–128.
- KIHIRA T, MIZUZAWA H, TADA J, NAMIKAWA T, YOSHIDA S, YASE Y (1993) Lewy body-like inclusions in Onuf's nucleus from two cases of sporadic amyotrophic lateral sclerosis. *Journal of the Neurological Sciences* **5**, 1–7.
- KIRBY R, FOWLER C, GOSLING J, BANNISTER R (1986) Urethrovaginal dysfunction in progressive autonomic failure with multiple system atrophy. *Journal of Neurology, Neurosurgery & Psychiatry* **49**, 554–562.
- KONISHI A, SATO M, MIZUNO M, ITO K, NOMURA S, SUGIMOTO T (1978) An electronmicroscope study of the area of Onuf's nucleus in the cat. *Brain Research* **156**, 333–338.
- KONNO H, YAMAMOTO T, IWASAKI Y, IZUKA H (1986) Shy-Drager syndrome and amyotrophic lateral sclerosis: cytoarchitectonic and morphometric studies autonomic neurones. *Journal of the Neurological Sciences* **73**, 193–204.
- KUZUHARA S, KANAYAWA I, NAKANISHI T (1980) Topographical localisation of the Onuf's nuclear neurons innervating the rectal and vesical striated sphincter muscles: a retrograde fluorescent double labelling in cat and dog. *Neuroscience Letters* **16**, 125–130.
- LAGERBACK PA (1985) An ultrastructural study of cat lumbosacral γ -motoneurons after retrograde labelling with horseradish peroxidase. *Journal of Comparative Neurology* **240**, 256–264.
- LAGERBACK PA, RONNEVI LO (1982) An ultrastructural study of serially sectioned Renshaw cells. II. Synaptic types. *Brain Research* **246**, 181–192.
- LAREULLE L (1937) La structure de la moelle épinière en coupes longitudinales. *Revue Neurologique* **67**, 695–711.
- LEEDY MG, BRESNAHAN JC, MAWE GM, BEATTIE MS (1988). Differences in synaptic inputs to preganglionic neurons in the dorsal and lateral band subdivisions of the cat sacral parasympathetic nucleus. *Journal of Comparative Neurology* **268**, 84–90.
- MANNEN T, IWATA M, TOYOKURA Y, NAGASHIMA K (1977) Preservation of a certain motoneuron group of the sacral spinal cord in amyotrophic sclerosis: its clinical significance. *Journal of Neurology, Neurosurgery and Psychiatry* **40**, 464–469.
- MAYHEW TM (1992) A review of recent advances in stereology for quantifying neural structure. *Journal of Neurocytology* **21**, 313–328.
- NAGASHIMA T, BEPPU M, UONO M, YAMADA H (1979) Demonstration of neuronal localisation of Onufrowicz's cell group X in rabbit by double labelling method. *Acta Histochemica et Cytochemica* **12**, 369–391.
- NAKAGAWA S (1980) Onuf's nucleus of the sacral cord in a South American monkey (Saimiri): its location and bilateral cortical input from area 4. *Brain Research* **191**, 337–344.
- ONUFROWICZ B (1889) Notes on the arrangement and function of the cell groups in the sacral region of the spinal cord. *Journal of Nervous and Mental Disorders* **26**, 498–504.
- ONUFROWICZ B (1890) On the arrangement and function of the cell groups of the sacral region of the sacral spinal cord in man. *Archives of Neurology and Psychopathology* **3**, 387–411.
- PAKKENBURG B, GUNDERSEN HJG (1988) Total number of neurons and glial cells in human brain nuclei estimated by the disector and the fractionator. *Journal of Microscopy* **150**, 1–20.
- PULLEN AH (1988) Quantitative synaptology of feline motoneurons to external anal sphincter muscle. *Journal of Comparative Neurology* **269**, 414–424.
- PULLEN AH, MARTIN JE (1995) Ultrastructural abnormalities with inclusions in Onuf's nucleus in motor neuron disease (amyotrophic lateral sclerosis). *Neuropathology and Applied Neurobiology* **21**, 327–340.
- PULLEN AH, MARTIN JE, SWASH M (1992) Ultrastructure of pre-synaptic input to motor neurons in Onuf's nucleus: controls and motor neuron disease. *Neuropathology and Applied Neurobiology* **18**, 213–231.
- REXED BA (1954) A cytoarchitectonic atlas on the spinal cord in the cat. *Journal of Comparative Neurology* **100**, 297–379.
- ROPPOLO JR, NADELHAFT I, DEGROAT WC (1985) The organization of pudendal motoneurons and primary afferent projections in the spinal cord of the Rhesus monkey revealed by horseradish peroxidase. *Journal of Comparative Neurology* **243**, 475–488.
- SASAKI S, MURAYAMA S (1993) A fine structural study of Onuf's nucleus in sporadic amyotrophic lateral sclerosis. *Journal of the Neurological Sciences* **119**, 28–37.
- SATO M, MIZUNO M, KONISHI (1978) A localisation of motoneurons

- innervating perineal muscles: a HRP study in cat. *Brain Research* **140**, 149–154.
- SCHRODER HD (1980) Organisation of the motoneurons innervating pelvic muscles of the male rat. *Journal of Comparative Neurology*, **192**, 567–587.
- SCHRODER HD (1981) Onuf's nucleus X: a morphological study of a human spinal nucleus. *Anatomy and Embryology* **162**, 443–453.
- SCHRODER HD (1984) Somatostatin in the caudal spinal cord: an immunohistological study of the spinal centres involved in the innervation of pelvic organs. *Journal of Comparative Neurology* **223**, 400–414.
- STERIO DC (1984) The unbiased estimation of number and sizes of arbitrary particles using the disector. *Journal of Microscopy* **134**, 127–136.
- STRICK PL, BURKE RE, KANDA K, KIM CD, WALMSLEY B (1976) Differences between alpha and gamma motoneurons labelled with horseradish peroxidase by retrograde transport. *Brain Research* **113**, 582–588.
- SUNG JH, MASTRI AE, SEGAL E (1979) Pathology of Shy-Drager syndrome. *Journal of Neuropathology and Experimental Neurology* **38**, 353–368.
- TAKAHASHI K, YAMAMOTO T (1979) Ultrastructure of the cell group X in the cat spinal cord. *Zellforschung und mikroskopische Anatomie Forschung (Leipzig)* **93**, 244–256.
- TASHIRO T, SADOTA T, MATSUSHIMA R, MIZUNO N (1989) Convergence of serotonin-, enkephalin- and substance P-like immunoreactive afferent fibres on single pudendal motoneurons in Onuf's nucleus of the cat: a light microscope study combining the triple immunocytochemical staining technique with the retrograde HRP-tracing method. *Brain Research* **481**, 392–398.
- TOMLINSON BE, IRVING D, REBEZ JJ (1973) Total numbers of limb motor neurons in the human lumbosacral cord and an analysis of the accuracy of various sampling procedures. *Journal of the Neurological Sciences* **20**, 313–327.
- THOR KB, MORGAN C, NADELHAFT I, HOUSTON M, DEGROAT WC (1989) Organisation of afferent and efferent pathways in the pudendal nerve of the female cat. *Journal of Comparative Neurology* **288**, 263–279.
- UEYAMA T, MIZUNO N, TAKAHASHI O, NOMURA S, ARAKAWA H, MATSUSHIMA R (1985) Central distribution of efferent and afferent components of the pudendal nerve in Macaque monkeys. *Journal of Comparative Neurology* **232**, 548–556.
- ULFHAKE B, KELLERTH J-O (1981 a) A quantitative light microscopic study of the dendrites of cat spinal α -motoneurons after intracellular staining with horseradish peroxidase. *Journal of Comparative Neurology* **202**, 571–584.
- ULFHAKE B, KELLERTH J-O (1981 b) A quantitative light microscopic study of the dendrites of cat spinal γ -motoneurons after intracellular staining with horseradish peroxidase. *Journal of Comparative Neurology* **202**, 585–596.